Available online at www.sciencedirect.com
SCIENCE DIRECT®
Journal of Sound and Vibration 291 (2006) 963–985
JOURNAL OF SOUND AND VIBRATION
www.elsevier.com/locate/jsvi

Comparison of different methods to couple nonlinear source descriptions in the time domain to linear system descriptions in the frequency domain—Application to a simple valveless one-cylinder cold engine ☆

F. Albertson[a,*], H. Bodén[b], J. Gilbert[c]

[a] *Ultra Technology Europe AB, Videum Science Park, 351 96 Växjö, Sweden*
[b] *The Marcus Wallenberg Laboratory for Sound and Vibration Research, KTH, Teknikringen 8, 100 44 Stockholm, Sweden*
[c] *Laboratoire d'Acoustique de l'Université du Maine, UMR CNRS 6613, IAM, Avenue Olivier Messiaen, 72085 Le Mans Cedex 9, France*

Received 20 February 2005; received in revised form 30 March 2005; accepted 4 July 2005
Available online 2 November 2005

Abstract

In duct acoustics the fundamental sound generating mechanisms must often be described by nonlinear time domain models. A linear frequency domain model is in many cases sufficient for describing the sound propagation in the connected duct system. This applies both for fluid machines such as IC-engines and compressors and for musical wind instruments. Methods for coupling a nonlinear source description to a linear system description have been proposed by several authors. In this paper some of those methods are compared concerning accuracy, calculation time and the possibility to perform parametric studies. The model problem used is a simple piston–restriction system connected to a linear system with varying complexity. The piston and restriction are considered as the source part and are modelled nonlinearly.

1. Introduction

To understand and solve noise problems it is essential to know the strength of the noise sources and understand how they interact with different surroundings. In this article the main focus will be on in-duct fluid-borne noise sources but the techniques discussed are also applicable to vibro-acoustic problems. The acoustic source-receiving system problem can be subdivided in a number of different ways.

The description of the source and the receiving (duct-) system can be obtained from a theoretical model or from measurements using a so-called black box model, where the model parameters are obtained from experiments. In many cases no theoretical model is available, which means that black box models are frequently used especially for source characterization. A review of methods for obtaining black box source data from measurements can be found in Ref. [1].

☆ Supported by EC-project grant no. BRPR CT97-0394.
*Corresponding author. Tel.: +46 470 29421.
E-mail address: fredrik.albertson@telia.com (F. Albertson).

0022-460X/$ - see front matter © 2005 Elsevier Ltd. All rights reserved.
doi:10.1016/j.jsv.2005.07.046

The models for the sources and the sound propagation in the receiving system can be linear or nonlinear. Here, linear and nonlinear simply refers to the structure of the equations that describe the acoustic behaviour. The linear models can be further divided into time-invariant and time-varying, which means that the operators or boundary conditions in the governing equations are either independent or dependent on time.

The analysis of the problem can be made either in the time domain or in the frequency domain. For linear time-invariant models, the analysis is preferably done by transforming the problem via a Fourier transform to the frequency domain. For nonlinear models the Fourier transform is not directly applicable and the problem should be analyzed in the time domain. It is quite frequently found that a linear frequency domain model is sufficient, or even the only available model, to describe the receiving system or system boundary condition while a nonlinear time domain model is needed to describe the source. This is usually called a hybrid linear/nonlinear model. Techniques for coupling the data from the linear frequency domain model to the nonlinear time domain model are needed. The comparison of a number of such techniques is the main purpose of the present paper.

The models used can also be one-dimensional, two-dimensional or three-dimensional depending on the geometry of the studied systems and on the frequency range of interest. For linear sources it is also possible to get an estimate of the degree of interaction between the source and the receiving system for different frequency ranges. This can be obtained via the Helmholtz number

$$He = kl, \tag{1}$$

where $k = \omega/c$ is the acoustic wavenumber, ω is the angular frequency, c is the speed of sound and l is a typical length scale for the acoustic propagation. In duct propagation problems, the length scale would typically be the duct radius. If He is much larger than one, the source will effectively behave as if the receiving system is infinite. It is then possible to use the acoustic power generated under free field conditions to characterize the source. When He is of the same order or smaller than unity the source behaviour is strongly influenced by the system boundaries. In this case sound power is not sufficient for describing the source and the one-port, two-port and multi-port models described in Ref. [1] must be used.

In the following discussion only one-dimensional low Helmholtz number applications will be included. Linear models for the source and the receiving system are frequently used. A number of references to in-duct applications and also some structure borne sound applications are given in Ref. [1]. The applications include clearly linear sources as ventilation fans but also IC-engine exhaust systems where the linearity of the source can be put in question. Methods for experimentally testing the linearity of a source under test are given in Ref. [2]. Many fluid machines such as compressors and IC-engines are high level acoustic sources. The validity of modelling them as linear time-invariant systems may therefore indeed be questioned. The alternative is of course to use nonlinear models to describe the complete system, see, e.g., Refs. [3,4]. The most important factor that determines the transition from linear to nonlinear models is the sound level in the system. As a first estimate it can be stated that if the relative pressure fluctuations caused by a machine is less than 1% the linear models are applicable. For air at standard conditions, this corresponds to sound pressure levels less than 150 dB (re. 20 mPa). It should be noted that this value applies to a propagating wave. Even in a small amplitude wave, it is possible that nonlinear effects can accumulate when the wave propagates a large number of wavelengths. This phenomenon is called shock wave formation and will occur if the losses are small enough [5]. Locally at, e.g., narrow constrictions in a system, nonlinearities can also occur at much lower levels. In the model problem used in this article only local nonlinearity will be considered, while shock wave formation is neglected.

Most works in this field have started from first principles, i.e., the equations describing the conservation of energy, momentum and mass in a fluid. To simplify the problem somewhat, lumped source models and 1-D sound propagation have often been assumed. The resulting equations are solved in the time domain using the method of characteristics or finite difference methods. The disadvantage of using these methods, compared to the linear frequency domain methods, is that they are more complicated to use and they cannot treat the complicated geometries found in, e.g., automobile silencers.

The hybrid linear/nonlinear methods, where a nonlinear time domain model is used for the source and a linear frequency domain model is used for the receiving system, was first introduced for in-duct sources in Refs. [6,7]. A frequency domain iterative one-point method was used to perform the coupling between the time

domain solution for the source and the frequency domain description of the rest of the system. The same technique was also suggested by Jones [3] for application to IC-engine exhaust systems and tested by Bodén [8] for a modified compressor with unstable results. The problem seems to be the chosen coupling technique even though acceptable results were obtained in Refs. [6,7]. The harmonic balance technique is an alternative frequency domain technique, using an Euler method instead of the one-point method, with better convergence properties. It has been used for microwave circuits in forced oscillations [9,10] and was adapted for modelling the self-sustained oscillations of wood-wind instruments by Gilbert et al. [11].

The hybrid methods can be divided into a number of main groups. One group is the iterative techniques, which can be further subdivided into frequency domain iterative techniques [6,7,9–12] and time domain iterative techniques [13] depending on in which domain the convergence check and the coupling is performed. Another group is the convolution techniques where the frequency domain impedance boundary condition is transformed into the time domain. The impedance boundary condition is given by

$$P(\omega) = Z(\omega)Q(\omega), \tag{2}$$

where $P(\omega)$ is the pressure at the boundary, $Z(\omega)$ is the impedance and $Q(\omega)$ is the flow velocity at the boundary. This equation can be transformed into the time domain giving

$$p(t) = \int_0^t z(t-\tau)q(\tau)\,\mathrm{d}\tau, \tag{3}$$

where $z(t)$ is the impulse response of the system with frequency response $Z(\omega)$. The convolution can be solved numerically which can be rather time consuming. It has also been reported that the impulse response convolution technique can give unstable results [14]. An alternative is to reformulate the boundary condition using the reflection coefficient $R(\omega)$, which can be calculated from the impedance by

$$R(\omega) = \frac{Z(\omega) - Z_c}{Z(\omega) + Z_c}, \tag{4}$$

where Z_c is the characteristic impedance. The boundary condition is then given by

$$P_-(\omega) = R(\omega)P_+(\omega), \tag{5}$$

where $P_+(\omega)$ and $P_-(\omega)$ are the amplitudes of the incident and reflected pressure waves at the boundary. The corresponding time domain expression is given by

$$p_-(t) = \int_0^t r(t-\tau)p_+(\tau)\,\mathrm{d}\tau, \tag{6}$$

where $r(t)$ is the reflection function of the system with reflection coefficient $R(\omega)$. The reflection function seems to give more stable results than the impulse response function. A reflection function convolution technique was used by Gazengel et al. [15], as well as a number of other authors in musical acoustics, for time domain simulation of single reed wind instruments. An impulse response convolution technique was suggested in Ref. [13] in conjunction with iteration. In some works on IC-engine exhaust and intake systems convolution using the reflection function [16,17] or scattering matrix [18,19] have been used. In these studies nonlinear wave propagation, calculated using the method of characteristics, in the exhaust pipe upstream of the linear boundary condition [16,17] or even in the pipes in-between mufflers [18,19] is an important part of the models. Since these techniques are not applicable to the model problem studied in this paper they will not be further considered. An impulse response convolution technique has also been suggested [20] for solving the problem of acoustic locally reacting impedance boundary conditions for computational aeroacoustics codes. For these codes computational efficiency is very important and the direct implementation of convolution according to Eq. (3) or (6) will be too time consuming. To solve this problem Eq. (3) is z-transformed giving,

$$P(z) = Z(z)Q(z). \tag{7}$$

The impedance $Z(z)$ is modelled as a IIR filter according to the equation

$$Z(z) = \frac{a_0 + \sum_{n=1}^{N} a_n z^{-n}}{1 - \sum_{k=1}^{K} b_k z^{-k}}, \tag{8}$$

where a_n and b_k are the filter coefficients that have to be identified from $Z(\omega)$ using digital-processing techniques. The resulting IIR-filtering can be implemented in the numerical codes in a computationally efficient way. A method close to the IIR filter is the expansion method proposed in Ref. [14], where the reflection coefficient in Eq. (4) is expanded into a stable differential operator.

In this paper the following methods are presented and tested: the Harmonic Balance Method with a Newton–Raphson step algorithm, a frequency domain iteration method with a one-point step algorithm, a time domain iteration method with a one-point step algorithm, a convolution method based on the reflection function and a convolution method based on the impulse response function. For completeness, a short description is given of an expansion method.

2. Description of model problem

The objectives are to study the features of different coupling methods. To this end, a simple model problem is chosen to simplify the modelling of the system and emphasize the coupling methods. This model problem should be easily described using simple nonlinear and linear equations. To satisfy the requirements, a simple piston–restriction system was chosen, see Fig. 1. This system is a compressor with the valve removed. Hence, no mean flow is present, but only an oscillating flow through the constriction.

The system is divided in two separate parts. These parts are connected over some chosen cross section. One part contains the linear part of the system, often a pipe system in applications, and the other part contains the nonlinear source part. Here only a brief summary of the model problem is given. See Ref. [12] for a detailed description.

On the left-hand side of Fig. 1 the simple piston–restriction system is depicted. A principal sketch of the same system is shown on the right-hand side of Fig. 1. Using the three volumes 1, 2 and 3, according to Fig. 1, the unknowns are defined as written below the principal sketch. A subscript denotes in which volume the unknown is given. Four quantities are studied, the pressures $p_1(t)$ and $p_3(t)$, the volume flow $q_3(t)$ and the density $\rho_1(t)$. A comprehensive derivation of the equations is given in Ref. [12]. Here, the equations are only summarized as follows. To emphasize the different domains, the time domain unknowns are written in lowercase letters, while the frequency domain unknowns are written with uppercase letters. The time domain equations of the model of the simple piston–restriction

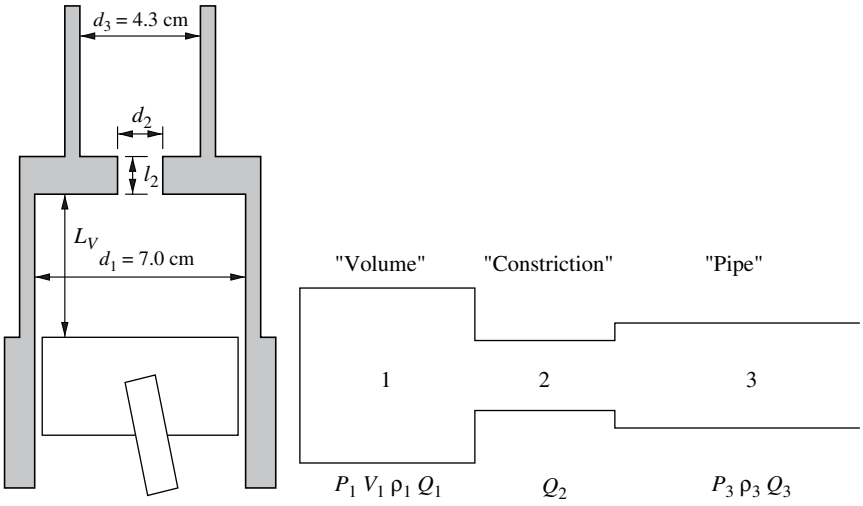

Fig. 1. The piston–restriction system used in the model. A one-dimensional approximation was used. The source volume is labelled volume 1, the constriction volume 2 and the pipe volume 3.

system are

$$p_1(t)-p_3(t)=\begin{cases}\dfrac{\rho_2}{2}q_3^2(t)\left(\dfrac{1}{S_2^2}-\dfrac{1}{S_1^2}\right)+\dfrac{\partial q_3}{\partial t}(t)\dfrac{\rho_2}{S_2}(\delta_1+l_2), & q_3(t)>0,\\ -\dfrac{\rho_2}{2}q_3^2(t)\left(\dfrac{1}{S_2^2}-\dfrac{1}{S_3^2}\right)+\dfrac{\partial q_3}{\partial t}(t)\dfrac{\rho_2}{S_2}(\delta_3+l_2), & q_3(t)<0,\end{cases} \tag{9}$$

$$\frac{\mathrm{d}}{\mathrm{d}t}(V_1(t)\rho_1(t))=-\rho_0 q_3(t), \tag{10}$$

$$p_1(t)=P_0(\rho_1(t)/\rho_0)^n \tag{11}$$

and finally the frequency domain equation is

$$Q_3(\omega)=Y_3(\omega)P_3(\omega) \quad \text{or} \quad P_3(\omega)=Z_3(\omega)Q_3(\omega). \tag{12}$$

Note that Eq. (9) is not symmetric. For different signs of the volume flow Q_3, different equations are applied. Except for the studied unknowns as defined above, the quantities in the equations are $\rho_0=\rho_2=1.23\,\mathrm{kg/m^3}$, $S_1=$ area of the pipe in volume 1, $S_2=$ area of the pipe in volume 2, $S_3=$ area of the pipe in volume 3, $\delta_1=$ acoustic end correction in volume 1, $\delta_3=$ acoustic end correction in volume 3, $l_2=$ length of constriction (see Fig. 1), $n=1.4$ is the polytropic index, $P_0=10^5\,\mathrm{Pa}$, while $Y_3(\omega)$ and $Z_3(\omega)$ are the admittance and impedance of the linear part of the system.

The oscillating volume $V_1(t)$ provides a driving force and is closely linked to the movement of the piston. From the piston geometry defined in Fig. 2 it is found that the oscillating volume is

$$V_1=S_1L_v+S_1L_{A1}\left(1+\cos(\omega t)+\frac{L_{A2}}{L_{A1}}\left[1-\sqrt{1-\left(\frac{L_{A1}}{L_{A2}}\right)^2\sin^2(\omega t)}\right]\right). \tag{13}$$

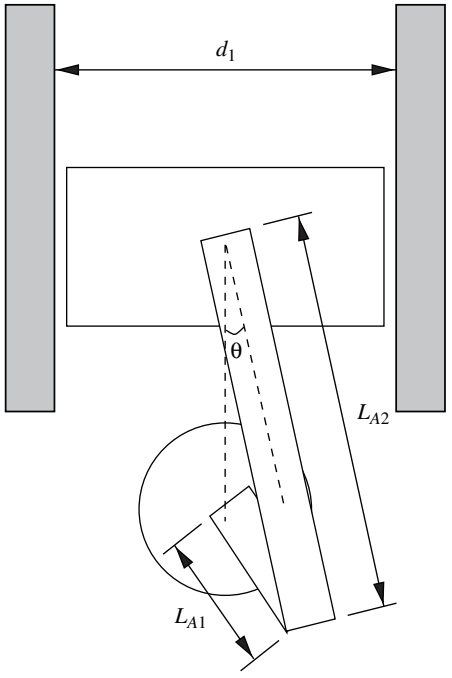

Fig. 2. Detailed picture of the piston movement. The angle $\theta=\omega t$ in Eq. (13). The fundamental frequency is constant given by $f_0=\omega_0/2\pi$, the rotational speed of the crankshaft. Here, $L_{A1}=40\,\mathrm{mm}$ and $L_{A2}=95\,\mathrm{mm}$.

Here $L_{A1} = 40\,\text{mm}$ and $L_{A2} = 95\,\text{mm}$ are the lengths of the axes as specified in Fig. 2, ω is the angular frequency, S_1 is the area of the pipe in volume 1 and L_v is the buffer length, i.e. the minimum length, from the piston to the constriction, see Fig. 1.

3. Iterative methods

All iteration methods are based on the same basic iteration concept. A convergence loop is constructed by choosing an order in which the equations are applied. The solution of the equations representing the system behaviour is found by iterating this convergence loop with different initial values. The final value of some specific unknown of the convergence loop is used as a parameter for changing the initial conditions, until some predefined convergence criteria is satisfied. The various methods differ in how this final value is used for modifying the initial values of the iteration. Another difference is in which regime the calculations are carried out.

A detailed description of the presented methods is given below. Note the differences in how the coupling is performed and furthermore in which domain the calculations are carried out. The general outline of the iteration process given above is also given for each iteration method.

3.1. Frequency domain hybrid methods

3.1.1. Harmonic balance method

The fundamental idea of the Harmonic Balance Method (HBM) is to "balance" or compare the N first harmonics in a series expansion. This also explains the name "Harmonic Balance Method". For this purpose, the studied system is decomposed into two separate subsystems, a linear and a nonlinear part. The linear part is treated in the frequency domain and the nonlinear part in the time domain. In the specific model problem of this paper, the nonlinear part is the source and the linear part is the (general) pipe system. The interface between the two subsystems consists of the Fourier transform pair. A comprehensive description together with a full reference list is given in Ref. [12].

A general outline of the HBM is as follows, see Fig. 3. First an appropriate unknown is chosen to use in the convergence check, which is performed in the frequency domain. After that, the equations are rewritten in a suitable form for a convergence loop. An initial value of the chosen unknown is given. The different linear and nonlinear equations are applied according to the convergence loop. Finally, a new value of the chosen convergence unknown is calculated. If the difference between the initial value and the final value of the first N harmonics satisfy the predefined convergence criteria, "harmonic balance" is reached. Otherwise, an increment of the initial value is calculated using a generalized Euler method, i.e. the Newton–Raphson method. The number of harmonics N used in the HBM has to be chosen by using some criterions. First, the amplitude of the Nth harmonic has to be much smaller than the dominating ones. Secondly, the total sound spectra must not change when the number of harmonics is changed.

For the specific model problem of the piston–restriction system, the convergence loop is defined as below. See Ref. [12] for a detailed description.

The HBM has earlier successfully been used for self-sustained oscillations of musical wind instruments [11]. The method was found to be very convenient for showing the modifications of the playing frequency and the spectrum when a physical parameter was changed or a new term was introduced in the equations.

In the applications given in Refs. [9,21] the HBM was used as a practical and effective method to analyze the steady-state periodic solutions based on the use of voltage and current probes of nonlinear microwave circuits. The stability of these steady-state periodic solutions was studied as well [10].

In Ref. [12] the HBM was applied, and thoroughly analyzed, for the same model problem as in this paper. A comprehensive study on the advantages, possibilities and drawbacks was presented together with several numerical examples.

In HBM, the FFT pair provides the interaction between the frequency domain and the time domain. In the direction from the time domain to the frequency domain the ordinary fast Fourier transform (FFT) is used. In the other direction, the frequency domain data is translated to a time domain series. That is, the inverse transformation is replaced by a sum of sines and cosines which converts the frequency domain data to time

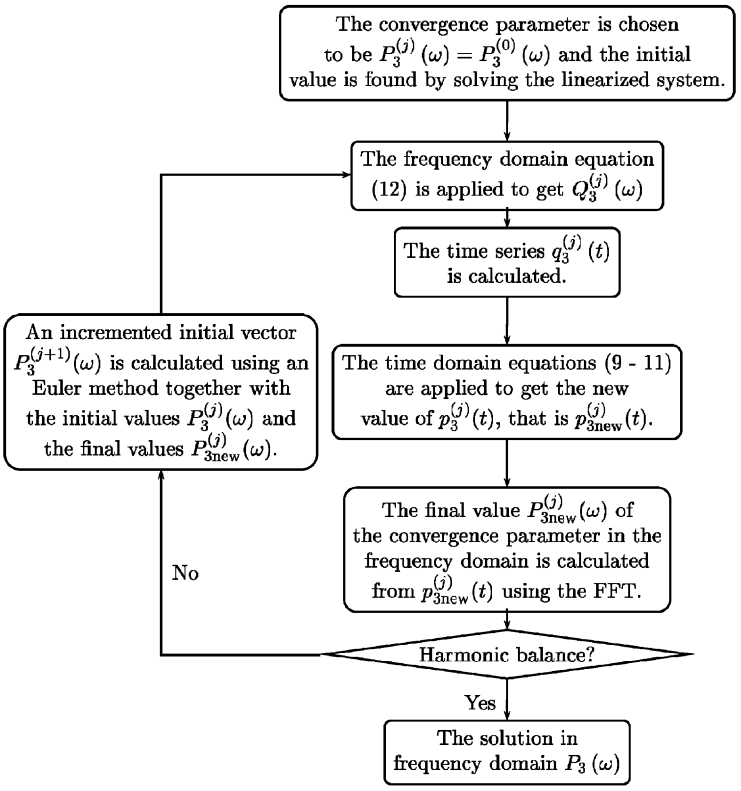

Fig. 3. Block diagram of the Harmonic Balance method with Euler coupling.

domain data. Here, it is assumed that only periodic functions are present, which is in line with the assumption of only studying steady-state periodic solutions. Let ω be the fundamental angular frequency and N the truncated number of harmonics considered. If $X(\omega) = \text{FFT}\{x\} = \{C_k\}$, where FFT means the Fast Fourier Transform, then

$$x(t) = \sum_{k=1}^{N} C_k e^{ik\omega t} = \sum_{k=1}^{N} [a_k \cos(k\omega t) + b_k \sin(k\omega t)], \tag{14}$$

where a_k and b_k are real while C_k is complex. The relation between a_k, b_k and C_k is given by

$$C_k = (a_k - ib_k)/2. \tag{15}$$

In the final equations of the model, the equations adopted to the HBM convergence loop, both integrals and derivatives are present. One of the advantages of the HBM is that it is very easy to integrate and differentiate.

3.1.2. One-point iteration method proposed by Soedel et al.

The iteration methods proposed by Soedel et al. in Refs. [4,6] are essentially equivalent to the piecewise HBM presented above. The main idea is similar, and all calculations from linear relations are carried out in the frequency domain. The difference between the two descriptions, as given in this paper, is the iteration process. Note that the two methods are both a "harmonic balance method", but here we distinguish between the methods in order to examine the effect of the coupling strategy. In HBM, the final value of the convergence parameter after the convergence loop is used for recalculating the initial value using an Euler method. Here, the new initial values are determined by simply inserting the final values as new initial values. That is, a one-point method is used. Since the difference between the initial and final values can be large, this means that the approach is more unstable.

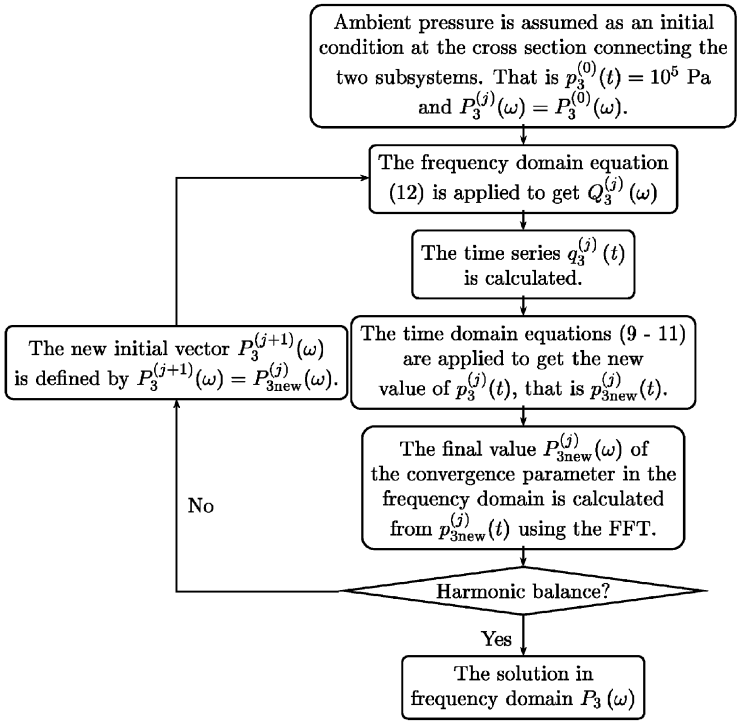

Fig. 4. Block diagram by Soedel et al. proposed Harmonic Balance method with one-point coupling.

The method is based on decomposition of equations in two subsystems, the linear part and the nonlinear part, over some cross section, and is applied as shown in Fig. 4.

Similar to the HBM, the Fourier transform pair provides the actual coupling between the time domain and the frequency domain. The ordinary FFT is used for transforming the time domain data to frequency domain data. For the transform back to the time domain, the inverse FFT is rewritten as a Fourier series, see Eq. (14). This works well only for periodic functions and it of course restricts the analysis to steady-state periodic solutions. Soedel et al. have later developed the method trying to stabilize the existing convergence problems [22]. The proposed method is to apply a convergence factor n in the equation

$$pa_i = n \cdot p_i + (1 - n) \cdot pa_{i-1}, \tag{16}$$

where pa_i is the pressure that is used in the final calculation stage, p_i is the pressure directly calculated in stage i and pa_{i-1} is the used pressure in stage $i - 1$.

3.2. Time domain methods

3.2.1. One-point iteration method proposed by Gupta et al.

In HBM [9–12] and the iteration method proposed by Soedel et al. [4,6], the computations are performed for only one complete cycle at a time. In the method proposed by Gupta [13], the impedance is transformed from the frequency domain to an equivalent time domain impedance boundary condition (TDIBC). The coupling is performed in the time domain using a convolution integral. The system time history, that is the past cycle data, is then used. There is thus a clear difference compared to the previous iteration methods.

The computational scheme is given in Fig. 5.

Note that the convolution is applied to a full cycle in each discrete time step. For this purpose, the data from the previous cycle is used. Mathematically, this can be expressed as follows. It is assumed that the convolution

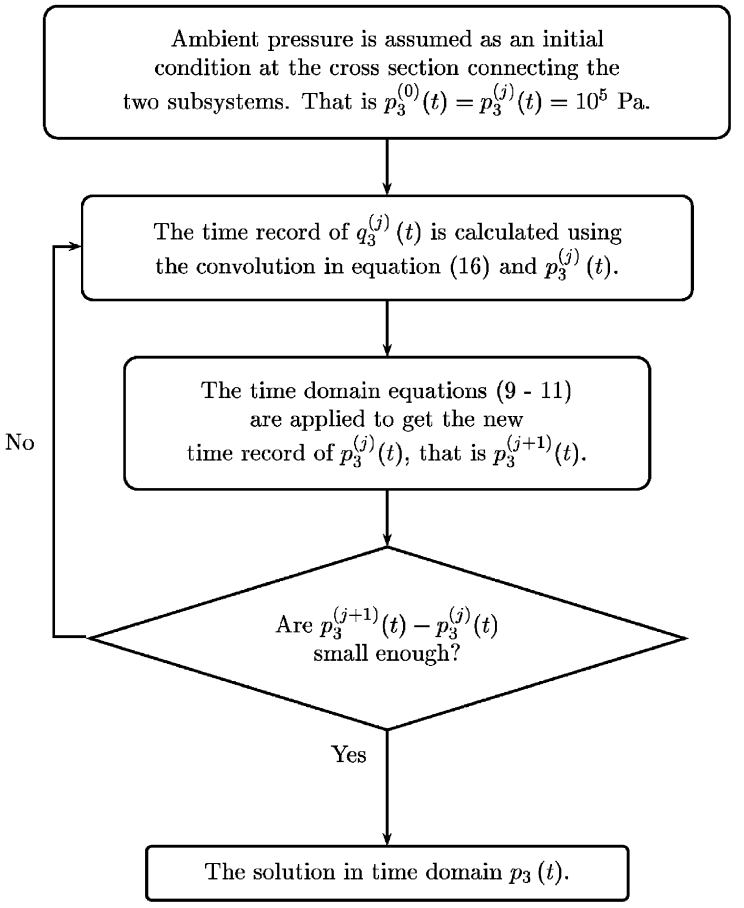

Fig. 5. Block diagram by Gupta et al. proposed time domain iterative method with one-point coupling.

is calculated using the time domain formulation of Eq. (12)

$$q_3(t) = y_3(t) * p_3(t) = \int_{\text{cycle}} y_3(\tau) \cdot p_3(t-\tau)\,\mathrm{d}\tau. \tag{17}$$

The number of samples used for the time vectors is N_s. The element number k in the vector q_3 for iteration $j+1$ is denoted

$$\{q_3\}_k^{j+1}. \tag{18}$$

Following the idea of Gupta [13], a new pressure vector $\{p_{3\text{new}}\}$ is defined by taking the last $N_s - k$ elements of the past pressure vector $\{p_3\}^j$ and the first k elements of the vector $\{p_3\}^{j+1}$. The convolution is then given by

$$\{q_3\}_{k+1}^{j+1} = \sum_{n=0}^{N_s} \{y_3\}_n \cdot \{p_{3\text{new}}\}_{N_s-n}. \tag{19}$$

4. Non-iterative methods

4.1. Convolution methods

A main drawback of the frequency domain iterative methods presented above, is that they are only adapted to calculate the steady-state periodic solutions. The time domain iteration method proposed by Gupta et al.

could in principle be used for finding transient behaviour, but the convergence criteria is the limiting factor. By nature a transient behaviour means changing behaviour, which implies that a solution cannot be found by using the present convergence criteria. On the contrary, the time domain methods are able to find the complete solutions including both transient and steady-state solutions. They are also well-adapted to finding solutions of problems where the control parameters change over time. Many of these methods have been used in musical acoustics [23,24] not only to find solutions of the model, but to do synthesis.

As with the iterative methods, the system is decomposed in two separate subsystems, a linear part and a nonlinear part. In the convolution method, the linear part is treated in the time domain as well. The impedance relation in Eq. (12) can be rewritten in the time domain as a convolution relation, where the impulse response $z(t)$ is the inverse Fourier transform of the impedance, see Eq. (3). The main drawback of this method thus becomes clear, since it is very time consuming to calculate the convolution integral as a long system memory is required. A way to minimize the time consumption is to apply a smaller time window for the convolution integral, see Table 1. One way to obtain this is to use a reflection function $r(t)$ in place of the impulse response $z(t)$. The reflection function is defined as the inverse Fourier transform of the plane wave reflection coefficient given in Eq. (4). The impulse response provides a relation between the acoustical pressure $p(t)$ and the acoustical volume flow $q(t)$ (or momentum flux), but the reflection function gives a relation between the incoming acoustical pressure $p_+(t)$ and the outgoing acoustical pressure $p_-(t)$ as described by Eq. (6). Note that the total pressure $p(t)$ is the sum

$$p(t) = p_+(t) + p_-(t) \tag{20}$$

and the volume flow $q(t)$ is given by

$$q(t) = \frac{p_+(t) - p_-(t)}{Z_c}. \tag{21}$$

The length of the time window can be significantly smaller for the reflection function compared to the impulse response. As an example the results for a open ended cylindrical pipe is shown in Fig. 6.

In the limit case of the lossless cylindrical tube, the corresponding reflection function is the negative dirac function with a delay $t_0 = 2L/c$ (twice the time of the "system length")

$$r(t) = -\delta(t - t_0) = -\delta(t - 2L/c). \tag{22}$$

If the thermoviscous losses are taken into account, there is a more complicated analytical reflection function [25]. Usually there is no analytical expression for the reflection function of realistic resonators like complex mufflers. But it can be calculated numerically from the geometry, see Fig. 7, using for example simulation softwares as SID [26]. The used muffler consists of one inlet and one outlet coupled together trough two parallel paths. The two paths include Helmholtz and quarterwave resonators, pipes, perforated pipes and absorptive material.

The difficulty of the technique is the development of the numerical tool which is reliable for low sampling frequencies. Each step of the numerical tool has to be studied very carefully. That is:

(1) the calculation of the discrete approximation of the plane wave reflection function,
(2) the description of the nonlinear source dynamics in the discrete time domain,
(3) solving the whole system.

Table 1
Time consumption for the open ended pipe case

Case	Time (s)
Convolution with reflection function	38.07
Convolution with impulse response (2 times length)	68.10
Convolution with impulse response (4 times length)	78.38
Harmonic Balance Method with Newton Raphson	8.73

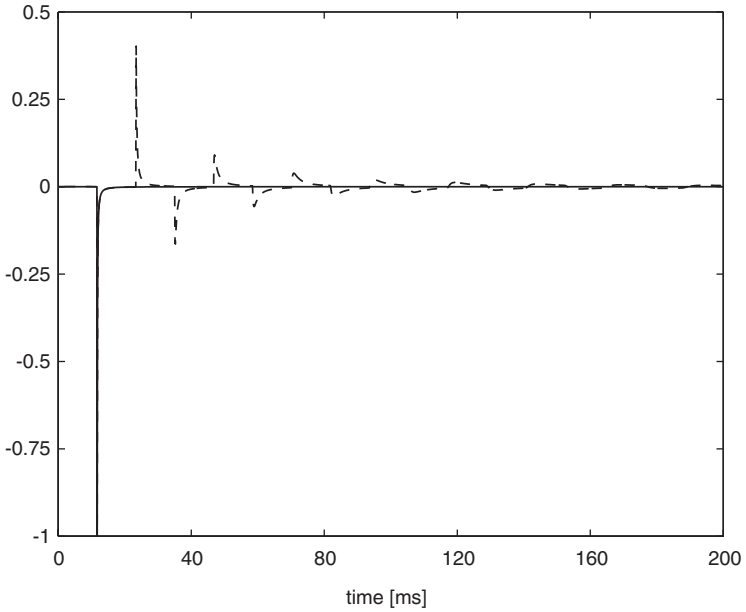

Fig. 6. The first 200 ms of the reflection function (solid) and the impulse response (dashed) of an open ended cylindrical pipe of 1.96 m length and 0.043 m diameter (calculations are including thermoviscous losses). Note that the graphs are rescaled to clearly show the differences.

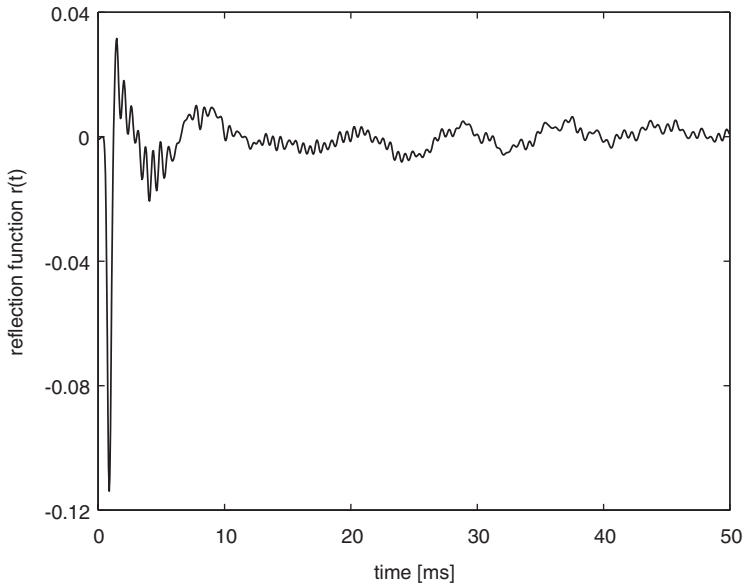

Fig. 7. The first 50 ms of the reflection function of a complex muffler (calculated numerically).

For an extensive discussion of these difficulties, and particularly about the discrete plane wave reflection function, see Ref. [15] where the time domain simulation of reed wind instrument behaviour is analyzed in detail. Below, points (2) and (3) applied to the compressor model problem (equations given in Section 2), are summarized.

The dynamics of the compressor model has been modelled by the three nonlinear equations (9–11). These equations are rewritten using two new variables y_1 and y_2 defined as

$$y_1(t) = \rho_1(t)V_1(t), \quad \text{and} \quad y_2(t) = q_3(t). \tag{23}$$

After the elimination of p_1 using Eq. (11), and the substitution of the variables $\rho_1 V_1$ and q_3 by y_1 and y_2, Eqs. (9) and (10) become a set of two ordinary nonlinear first-order differential equations as follows. For y_1 the differential equation is

$$\frac{\mathrm{d}y_1}{\mathrm{d}t} = -\rho_0 y_2. \tag{24}$$

For $q_3 = y_2 > 0$

$$\frac{\mathrm{d}y_2}{\mathrm{d}t} = \left[P_0 \left(\frac{y_1}{V_1 \rho_0} \right)^n - p_3 - P_0 - \frac{\rho_0}{2} \left(\frac{1}{S_2^2} - \frac{1}{S_1^2} \right) y_2^2 \right] \frac{S_2}{\rho_0 (l_2 + \delta_1)} \tag{25}$$

and for $q_3 = y_2 < 0$

$$\frac{\mathrm{d}y_2}{\mathrm{d}t} = \left[P_0 \left(\frac{y_1}{V_1 \rho_0} \right)^n - p_3 - P_0 + \frac{\rho_0}{2} \left(\frac{1}{S_2^2} - \frac{1}{S_3^2} \right) y_2^2 \right] \frac{S_2}{\rho_0 (l_2 + \delta_3)}. \tag{26}$$

These ordinary nonlinear differential equations are solved using an Adams–Bashforth, Adams–Moulton (ABAM) predictor–corrector numerical method. Before doing this, the last unknown variable p_3 remaining in the above equations has to be estimated.

If the impulse response method was used, p_3 would be directly related to y_2 by Eq. (23). Since the reflection function method is used, some straightforward algebra is needed to rewrite Eq. (5) to relate p_3 and q_3. Using Eqs. (20–21) applied to p_3 in place of p gives

$$2p_+ = p_3 + Z_c q_3 \tag{27}$$

and consequently

$$p_3 = p_+ + p_- = \frac{(p_3 + Z_c q_3) + r \cdot (p_3 + Z_c q_3)}{2} = \frac{(p_3 + Z_c q_3) + p_3^{\mathrm{past}}}{2}, \tag{28}$$

where p_3^{past} means the pressure p_3 due to the system history. That is, all system reflections are gathered into the past pressure. In the discrete time domain, $p_3[n]$ is calculated in the sample n (time sampling) assuming that every variable is known from sample 1 to sample $n-1$. Then Eq. (28) can be rewritten in the discrete time domain as

$$p_3^{\mathrm{past}}[n] = \sum_{k=1}^{n} r_d[k] \{ p_3[n-k] + Z_c q_3[n-k] \}, \quad r_d[0] = 0. \tag{29}$$

Note that $q_3 = y_2$.

The method of simulation described above to solve the whole system can be summarized as depicted in Fig. 8.

4.2. Expansion method

Fung et al. [14] have proposed yet another method. The main idea is to expand the impedance $Z(\omega)$ in powers of $(\mathrm{i}\omega)^k$ and then invert the series to a time domain linear operator, since the inverse Fourier transform of $(\mathrm{i}\omega)^k$ is $\mathrm{d}^k/\mathrm{d}t^k$. It is however found that a direct inversion of the power series of the impedance $Z(\omega)$ in general corresponds to an unstable differential operator. A direct inversion of the power series of the reflection coefficient $R(\omega)$ is claimed to give numerically stable, accurate and easily implementable results.

The reflection coefficient $R(\omega)$ is thus expanded into a power series as

$$R(\omega) = U + \mathrm{i}V = (U_0 + U_2\omega^2 + \cdots) + \mathrm{i}(V_1\omega - V_3\omega^3 + \cdots). \tag{30}$$

The linear differential operator is found by direct inversion of this power series. That is

$$r(t) = \left(U_0 - U_2 \frac{\mathrm{d}^2}{\mathrm{d}t^2} + \cdots \right) + \mathrm{i} \left(V_1 \frac{\mathrm{d}}{\mathrm{d}t} - V_3 \frac{\mathrm{d}^3}{\mathrm{d}t^3} + \cdots \right). \tag{31}$$

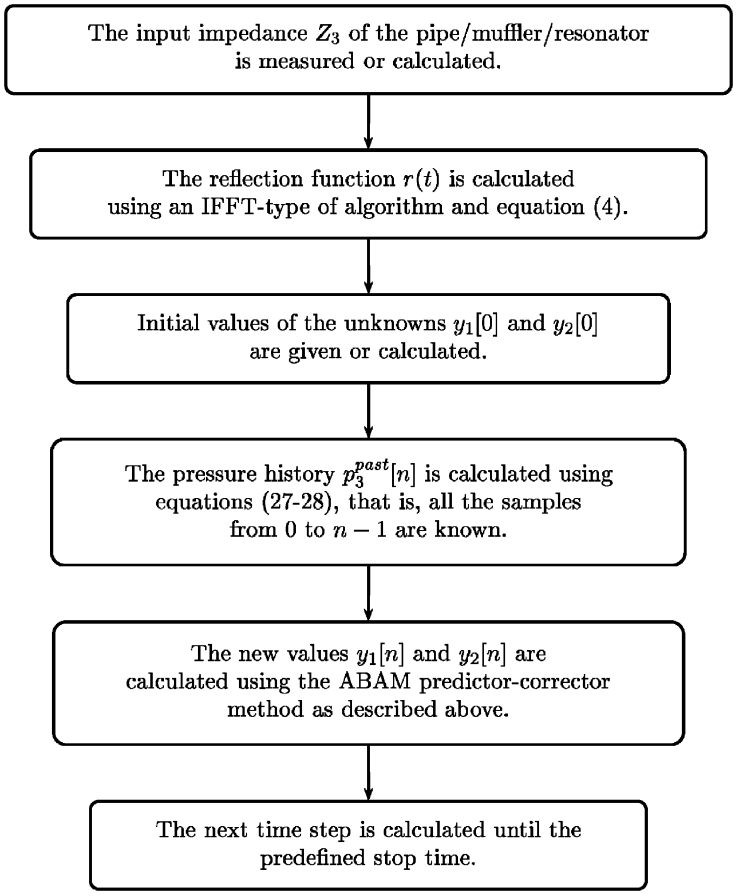

Fig. 8. Block diagram of the convolution method with reflection function.

Eq. (28) holds here as well. The only difference is that the expression of the past pressure $p_3^{\text{past}}(t)$ is replaced by

$$\begin{aligned} p_3^{\text{past}}(t) = U_0 &\int_0^t p_3(t-\tau) + Z_c q_3(t-\tau)\,\mathrm{d}\tau \\ &+ \sum_{k=1}^{n} (-1)^k U_{2k} \int_0^t \frac{\mathrm{d}^{2k}}{\mathrm{d}\tau^{2k}} [p_3(t-\tau) + Z_c q_3(t-\tau)]\,\mathrm{d}\tau \\ &+ \sum_{k=0}^{n} (-1)^k V_{2k+1} \int_0^t \frac{\mathrm{d}^{2k+1}}{\mathrm{d}\tau^{2k+1}} [p_3(t-\tau) + Z_c q_3(t-\tau)]\,\mathrm{d}\tau. \end{aligned} \tag{32}$$

By calculating the integrals it is found that the past pressure of $p_3^{\text{past}}(t)$ can be replaced by the following integro-differential operator.

$$\begin{aligned} p_3^{\text{past}}(t) = U_0 &\int_0^t p_3(t-\tau) + Z_c q_3(t-\tau)\,\mathrm{d}\tau - V_1[p_3(t) + Z_c q_3(t)] \\ &- \sum_{k=1}^{n} (-1)^k \left(U_{2k} \frac{\mathrm{d}^{2k-1}}{\mathrm{d}t^{2k-1}} + V_{2k+1} \frac{\mathrm{d}^{2k}}{\mathrm{d}t^{2k}} \right) [p_3(t) + Z_c q_3(t)]. \end{aligned} \tag{33}$$

Using this expression together with Eqs. (9–12) and Eq. (28) gives a new differential equation system which can be solved using some appropriate numerical method.

5. Comparison of coupling methods

A total of four methods have been tested: the HBM, the one-point iteration method in the frequency domain, the one-point iteration method in the time domain and the convolution method with a reflection function. The two one-point iteration methods gave unstable results for almost all test cases, while the HBM and the reflection function method gave in almost all cases stable results.

As a general conclusion it can be deduced that the one-point iteration methods give divergent solutions to a larger extent than the HBM, see Fig. 9. The reason is the main difference of the methods, namely the recoupling of the final value. In the one-point iteration methods the final value of a convergence loop is used as a new initial condition in the next loop. This one-point approach can cause divergent behaviour for systems where the initial condition is far away from the final solution. A better approach is to use the Newton–Raphson method used in the HBM. There the final value of a convergence loop is used for modifying the former initial condition. This gives smaller variations in the initial condition, and in many cases convergence where the one-point methods give divergent solutions.

The two better methods, that is the harmonic balance method and the convolution method with reflection function, have been compared for several cases. The comparison cases were chosen to give an increased complexity of the problem ranging from the easiest case with an infinite pipe to a more difficult case with a general impedance for a muffler.

Various features, for example time consumption and consistency between methods, are considered. Both the steady state as well as transient behaviours are studied. To this end, the following test cases were applied for the receiving part:

(i) infinite cylindrical pipes
(ii) finite cylindrical pipes
(iii) expansion chambers
(iv) complex commercial mufflers

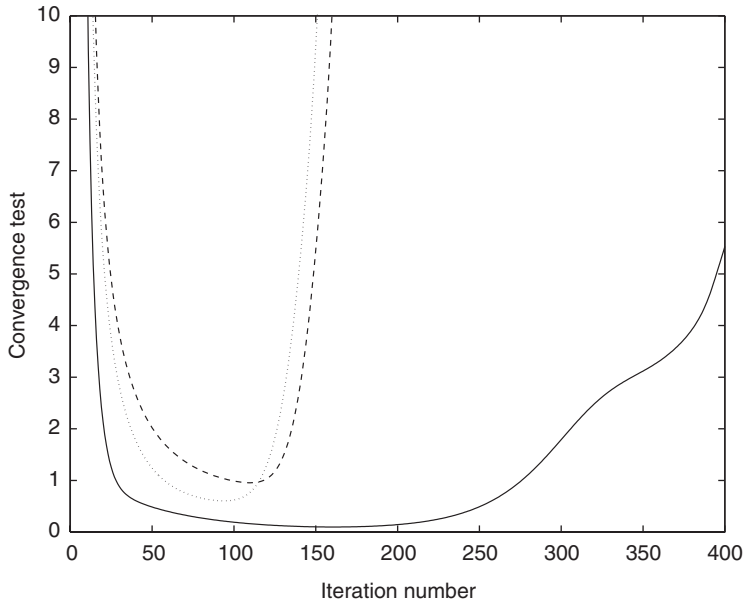

Fig. 9. The convergence test for the method proposed by Soedel et al. The fundamental frequency f_0 was 10 Hz, the diameter of the restriction was $d_2 = 3$ cm and the resonator was an open ended pipe of 1 m. The buffer length was $L_v = 36$ cm (solid), $L_v = 16$ cm (dashed) and $L_v = 6$ cm (dotted).

The source parameters (fundamental frequency f_0, buffer length L_v and orifice diameter d_2) were varied for all test cases. Finally, the transient behaviour of the system was analyzed by two different types of accelerations.

5.1. Steady-state solutions

5.1.1. Cylindrical pipes

First the case of infinite cylindrical pipes was used for comparison. In this case, the convolution integral reduces to

$$p_3(t) = Z_c q_3(t), \tag{34}$$

and consequently no pressure history has to be used in the calculations. The HBM and the reflection function method was compared for different values of the driving frequency f_0, the buffer length L_v and the orifice diameter d_2. In Fig. 10, the first ten harmonics of the sound pressure levels of $P_3(\omega)$ are plotted. In this case, the geometrical configuration is kept constant, but the frequency f_0 of the piston is altered (10 and 100 Hz). Note that there are actually two curves plotted. It is thus in practice no difference between the solution from HBM and the reflection function method in this case.

Figs. 11 and 12 show the volume flow $Q_3(t)$ and the density $\rho_1(t)$ for the infinite pipe case as well. Here different geometrical parameters are varied, while the frequency is held constant. Only on the left-hand side in Fig. 12, there is a very slight difference between the solutions from the different methods. The considered case of an infinite pipe is however the least complicated case, since no conversion between the impedance $Z_3(\omega)$ and the reflection function $r(t)$ has to be done. The general conclusion to be drawn must therefore be that it is a good sign that there is excellent agreement for this simple case.

A cylindrical pipe or a complex muffler has to be represented well in both the frequency domain and the time domain, to form a basis of the comparison of methods. It is important that the frequency domain representation and the time domain representation reflect the same physical system. Fig. 13 shows the reflection function $r(t)$ in the time domain and the admittance $Y_3(\omega)$ in the frequency domain for the same complex muffler. The admittance is adapted to fit the HBM, with values only at the harmonics. For 40 harmonics, only 40 values are needed.

In the reflection function a value for each time sample is needed. Consequently, the length of the reflection function is inversely proportional to the time step. The numerical predictor–corrector method used in this paper needs a fine mesh, that is a short time step, to produce accurate numerical solutions. This implies though

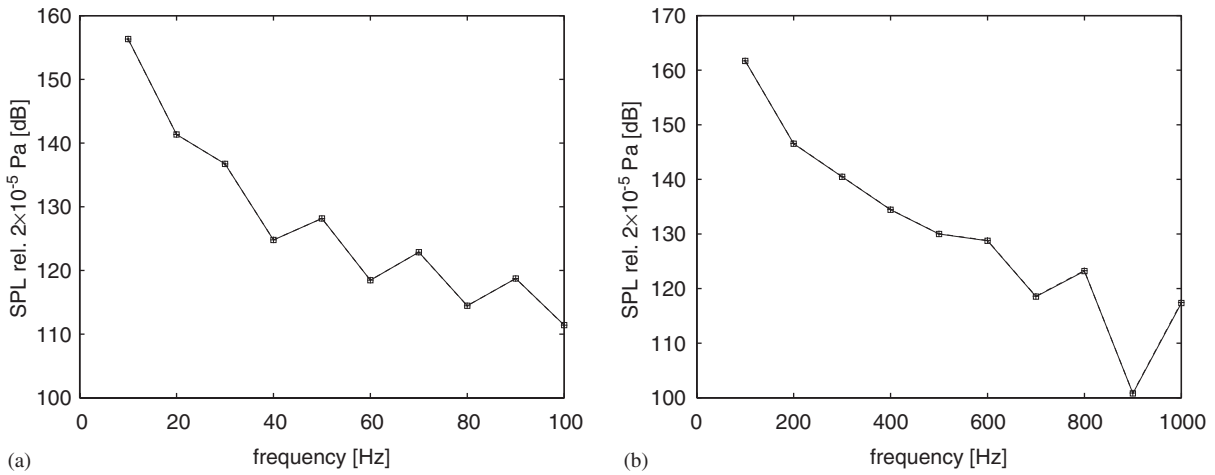

Fig. 10. Sound pressure level of $P_3(\omega)$ as a function of harmonics displayed in Hz. The resonator was an infinite pipe with 0.043 m diameter, the buffer length was $L_v = 16$ cm and the diameter of the restriction was $d_2 = 1$ cm. The HBM results (solid) and the reflection function method results (dashed) are so close that they are indistinguishable. (a) $f_0 = 10$ Hz; (b) $f_0 = 100$ Hz.

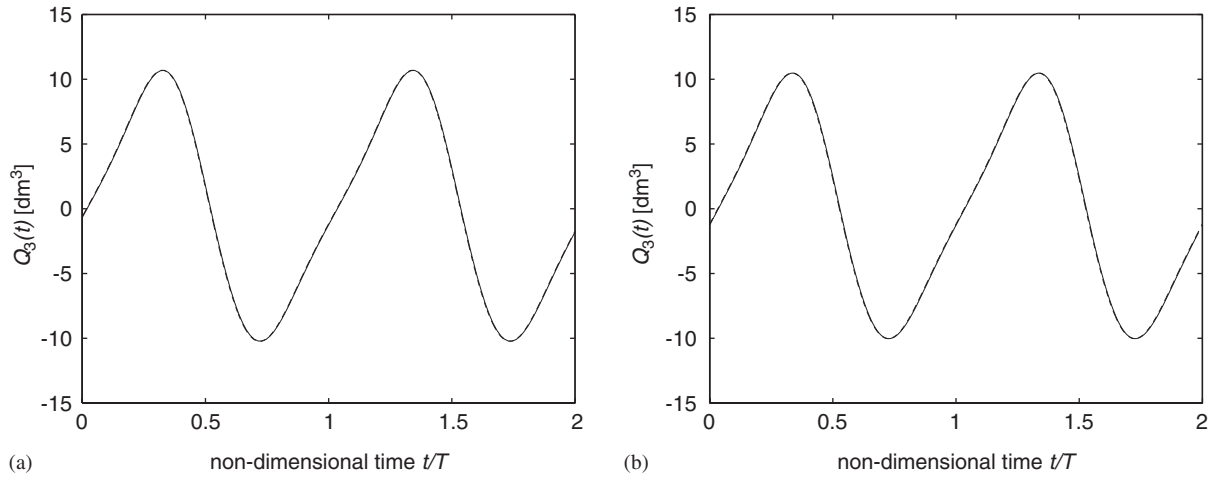

Fig. 11. Two periods of the volume flow $Q_3(t)$ in [dm^3] as a function of non-dimensional time t/T. The resonator was an infinite pipe with 0.043 m diameter, the fundamental frequency was $f_0 = 10$ Hz and the diameter of the restriction was $d_2 = 3$ cm. The HBM results (solid) and the reflection function method results (dashed) are so close that they are indistinguishable. (a) $L_v = 16$ cm; (b) $L_v = 36$ cm.

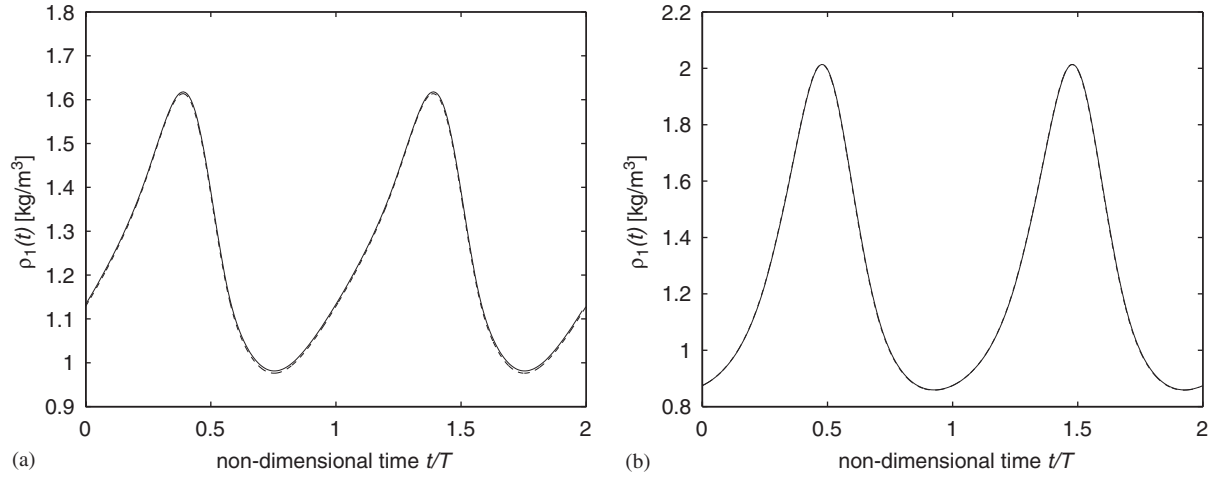

Fig. 12. Two periods of the density $\rho_1(t)$ in [kg/m^3] as a function of non-dimensional time t/T. The resonator was an infinite pipe with 0.043 m diameter, the fundamental frequency was $f_0 = 100$ Hz and the buffer length was $L_v = 6$ cm. The HBM results (solid) and the reflection function method results (dashed) are so close that they are indistinguishable. (a) $d_2 = 3$ cm; (b) $d_2 = 1$ cm.

a high sampling frequency F_s, since the time step is

$$\mathrm{d}t = \frac{2}{F_s}. \tag{35}$$

Here, one problem becomes obvious. A good description of the muffler is needed for high sampling frequencies in order to create a sufficient small time step. In Ref. [15] this problem is addressed and a number of possible solutions are discussed. Here, a linear FIR-filter is used together with phase-rotation and a time compensation for the filter as well as the rotation.

In comparing the length of the reflection function, that is the system time history needed, with the values in the harmonics for HBM, some conclusions about the calculation time are in place. The HBM solution was calculated more or less 15 times faster than the reflection function method. It is therefore suitable to use the HBM in cases where a lot of parametric studies are performed. An advantage of the HBM compared to the

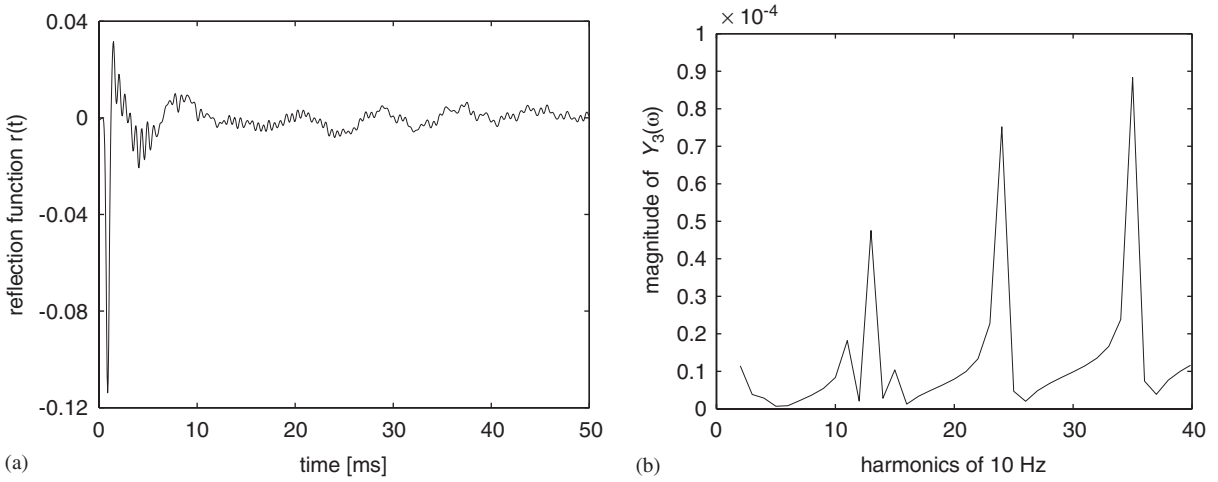

Fig. 13. A complex muffler represented by both the reflection function and the admittance. (a) Reflection function; (b) admittance.

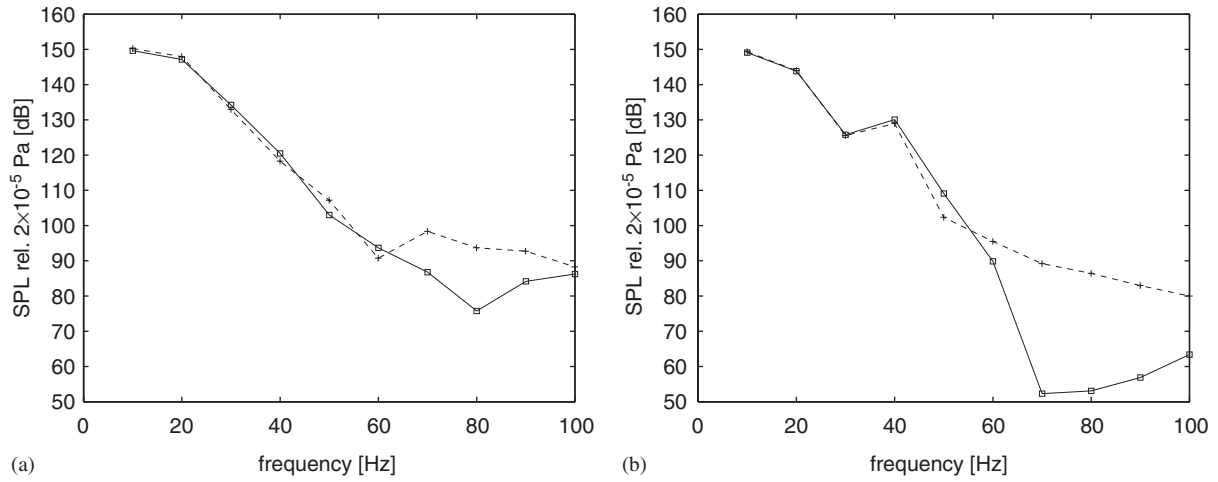

Fig. 14. Sound pressure level of $P_3(\omega)$ as a function of harmonics displayed in Hz. The resonator was an open pipe with 1.96 m length and 0.043 m diameter, the diameter of the restriction was $d_2 = 3$ cm and the fundamental frequency $f_0 = 10$ Hz. The HBM results (solid) and the reflection function method results (dashed) are displayed in the same figure. (a) $L_v = 36$ cm; (b) $L_v = 6$ cm.

reflection function method is also that previous solutions can be used as initial values to decrease the number of iterations. In the reflection function method, every calculation is restarted. A previous solution can of course give new initial values, but there is always a diminishing transient solution present.

As a next step, the complexity of the comparison cases was increased to examine how the methods reacted to different complexity and different variations. The infinite pipe configuration was switched to an open cylindrical pipe configuration. Here the problem of conversion between the impedance $Z_3(\omega)$ and the reflection function $r(t)$ are present. In Fig. 14 only the buffer length L_v is varied. On the right-hand side, $L_v = 6$ cm, which represents a more nonlinear case than the graph on the left-hand side, where $L_v = 36$ cm. The two methods give very similar results for the first four or six harmonics, but the solutions deviate for higher harmonics. Note that the level in the region of deviation is approximately 50–60 dB lower than the strongest harmonic.

Fig. 15 shows the reaction to variation in orifice diameter d_2. In this case, there is a very good agreement for $d_2 = 3$ cm, but a slight difference is present for $d_2 = 1$ cm. The decrease of orifice diameter represents an

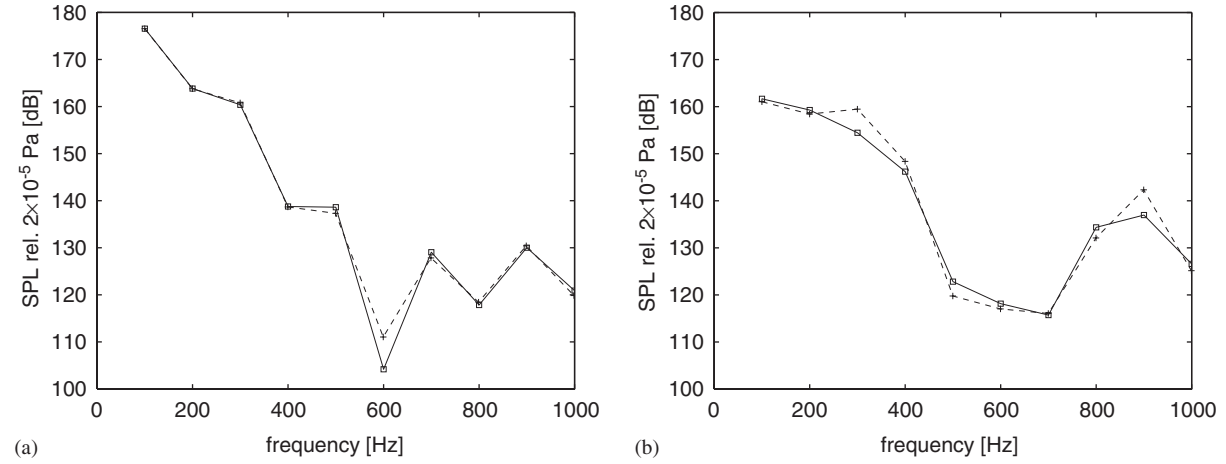

Fig. 15. Sound pressure level of $P_3(\omega)$ as a function of harmonics displayed in Hz. The resonator was an open pipe with 1.96 m length and 0.043 m diameter, the buffer length was $L_v = 6$ cm and the fundamental frequency $f_0 = 100$ Hz. The HBM results (solid) and the reflection function method results (dashed) are displayed in the same figure. (a) $d_2 = 3$ cm; (b) $d_2 = 1$ cm.

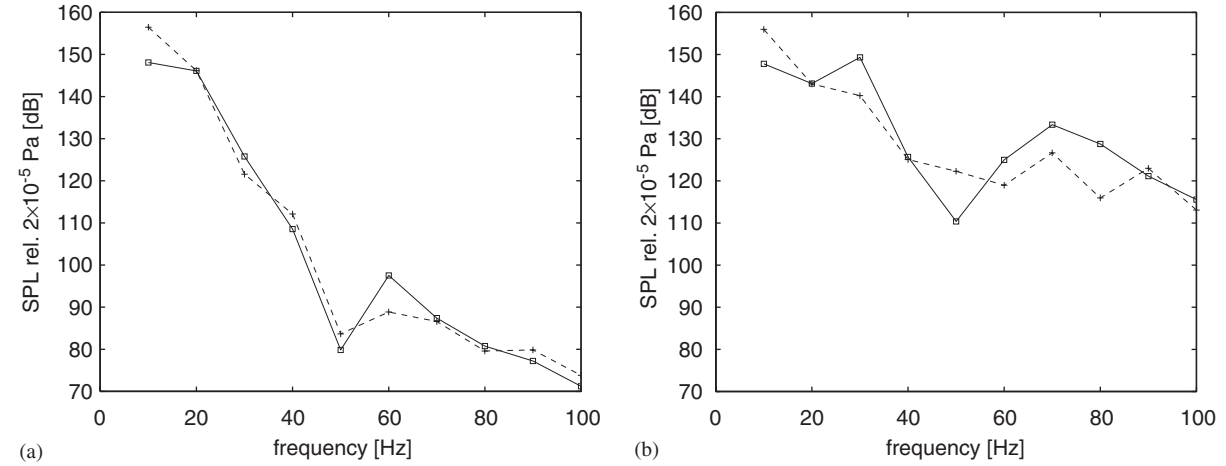

Fig. 16. Sound pressure level of $P_3(\omega)$ as a function of harmonics displayed in Hz. The resonator was an expansion chamber. The buffer length was $L_v = 16$ cm and the fundamental frequency $f_0 = 10$ Hz. The HBM results (solid) and the reflection function method results (dashed) are displayed in the same figure. (a) $d_2 = 3$ cm; (b) $d_2 = 1$ cm.

increase in nonlinearity of the system. From Figs. 14 and 15 it seems that the solutions differ more for a more nonlinear configuration of the system than for a more linear system.

5.1.2. *Mufflers*

Mufflers can be very complicated. To study the reaction of the solutions when complex mufflers are applied, two steps of complexity were used. First a simple expansion chamber was used, and then a plane wave model for a complex commercial muffler was used.

In Fig. 16, the sound pressure level of $P_3(\omega)$ is plotted. The degree of nonlinearity was increased by decreasing the orifice diameter d_2. While there is a fairly good agreement between the HBM and the reflection function solutions for $d_2 = 3$ cm, a larger deviation is visible for $d_2 = 1$ cm. This furthermore amplifies the preliminary conclusion that the methods produce slightly different solutions for a heavily nonlinear system.

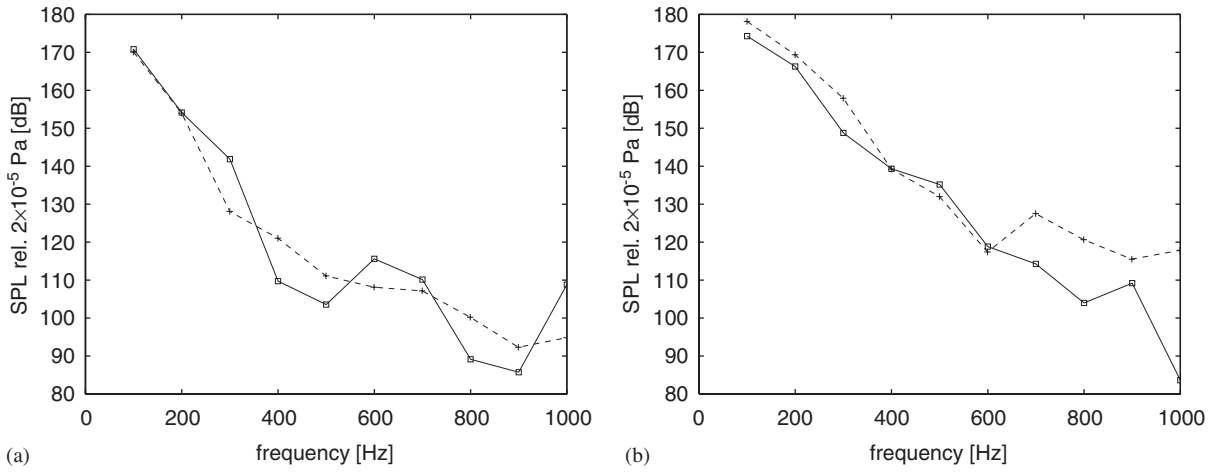

Fig. 17. Sound pressure level of $P_3(\omega)$ as a function of harmonics displayed in Hz. The resonator was an expansion chamber. The diameter of the restriction was $d_2 = 3$ cm and the fundamental frequency $f_0 = 100$ Hz. The HBM results (solid) and the reflection function method results (dashed) are displayed in the same figure. (a) $L_v = 36$ cm; (b) $L_v = 6$ cm.

Note that the y-axis has been rescaled to be equivalent in both graphs to clearly show the difference between the two cases.

In Fig. 17 the buffer length L_v is varied. The smaller value of L_v, that is a shorter buffer length, gives higher levels in the system. This is also clearly visible in comparing the graphs in the figure. The tendency in the graphs changing L_v was not clear, but a rather random pattern was found.

The commercial muffler was modelled by the simulation software SID [26], and the results from the software was compared with measurements with very good agreement for low frequencies. Fig. 18 shows four graphs with different values of the buffer length L_v. The first two graphs actually show very good agreement between the solutions from the two methods. The last two graphs though indicate that for a higher level, the accuracy is lower.

Finally, the worst found case is shown in Fig. 19. Here a change (rather large though!) in orifice diameter caused a major discrepancy between the solutions.

5.2. Transient solutions

Transient solutions are of great interest in industrial applications, for example in a car or truck acceleration. In this section, the abilities of the methods to model transient behaviour are analyzed.

For the HBM, the only type of solution that can be found is steady state and periodic. A so-called envelope method has though been proposed [27] to simulate a transient behaviour. The steady-state solution is calculated for each chosen driving frequency, for example a number of frequencies between 10 and 20 Hz as depicted in Fig. 20. Then the steady-state solutions are plotted in time domain or frequency domain for each calculated fundamental frequency. From this type of graph it is possible to deduce some physical properties of the system. On the left-hand side of Fig. 20 the graph shows the pressure $p_3(t)$ as a function of both time and fundamental frequency f_0. The red colour means high pressure and the blue means low pressure. On the right-hand side a close-up is shown. The pressure $p_3(t)$ is calculated for $d_2 = 3$ cm and $L_v = 16$ cm, while the linear part of the system was represented by the complex muffler used in the previous section, see Fig. 13 for reflection function and admittance of the muffler. For this set of parameters, the system seems to have a resonance at approximately 18.25 Hz. This is crucial knowledge for designing an efficient muffler.

However, an envelope method cannot really show the system behaviour during an acceleration, only reveal the resonances and other similar type of features of the system. The main reason for this is that when a system parameter is changed, the system will produce a particular solution to the differential equation system. In an HBM-based envelope method, all these transient system responses are missing, since only steady-state

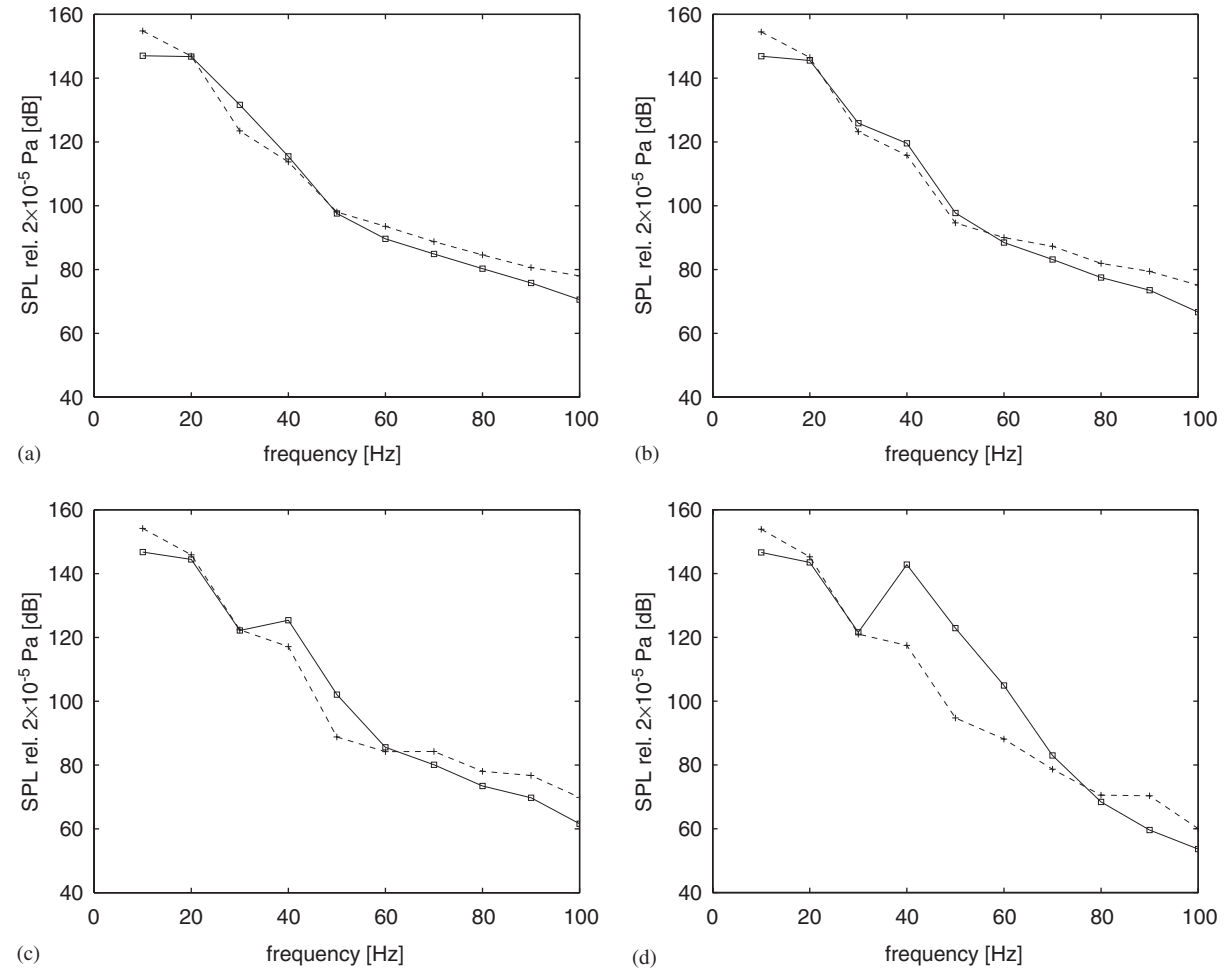

Fig. 18. Sound pressure level of $P_3(\omega)$ as a function of harmonics displayed in Hz. The resonator was a complex muffler. The diameter of the restriction was $d_2 = 3\,\text{cm}$ and the fundamental frequency $f_0 = 10\,\text{Hz}$. The HBM results (solid) and the reflection function method results (dashed) are displayed in the same figure. (a) $L_v = 36\,\text{cm}$; (b) $L_v = 26\,\text{cm}$; (c) $L_v = 16\,\text{cm}$; (d) $L_v = 6\,\text{cm}$.

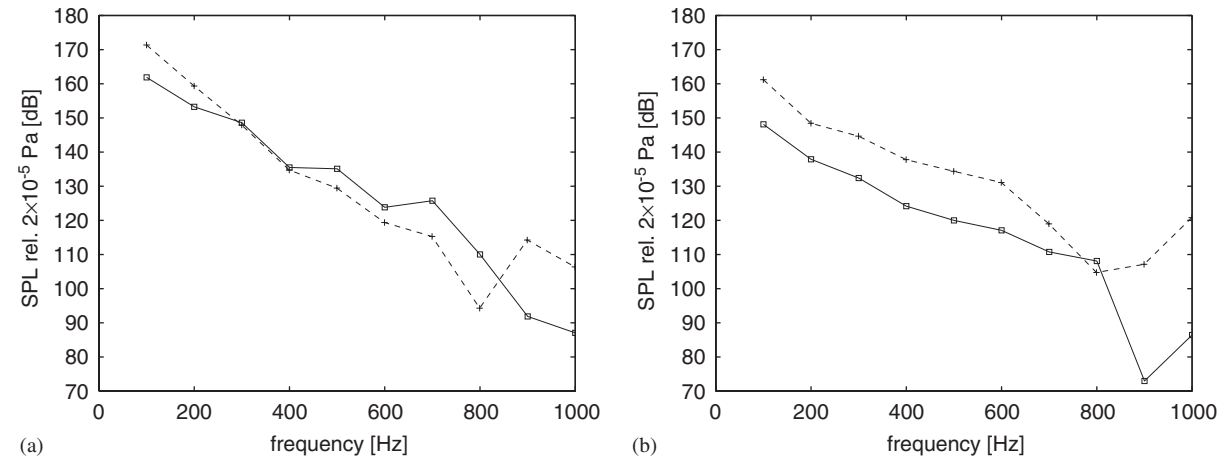

Fig. 19. Sound pressure level of $P_3(\omega)$ as a function of harmonics displayed in Hz. The resonator was a complex muffler. The buffer length was $L_v = 16\,\text{cm}$ and the fundamental frequency $f_0 = 100\,\text{Hz}$. The HBM results (solid) and the reflection function method results (dashed) are displayed in the same figure. (a) $d_2 = 3\,\text{cm}$; (b) $d_2 = 1\,\text{cm}$.

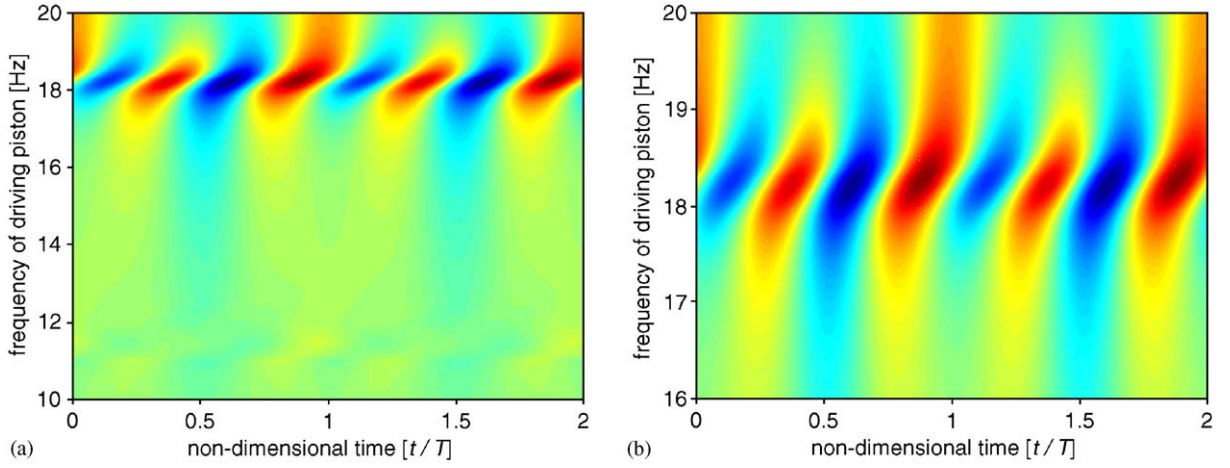

Fig. 20. The HBM-based envelope of the sound pressure $p_3(t)$ plotted as a function of both non-dimensional time and fundamental frequency. The scale is blue for low pressures, then green, yellow and finally red for high pressures. The resonator was a complex muffler. The buffer length was $L_v = 16\,\text{cm}$ and the diameter of the restriction was $d_2 = 3\,\text{cm}$. Note that the fundamental frequency is altered from 10 to 20 Hz. (a) 10–20 Hz; (b) 16–20 Hz close-up.

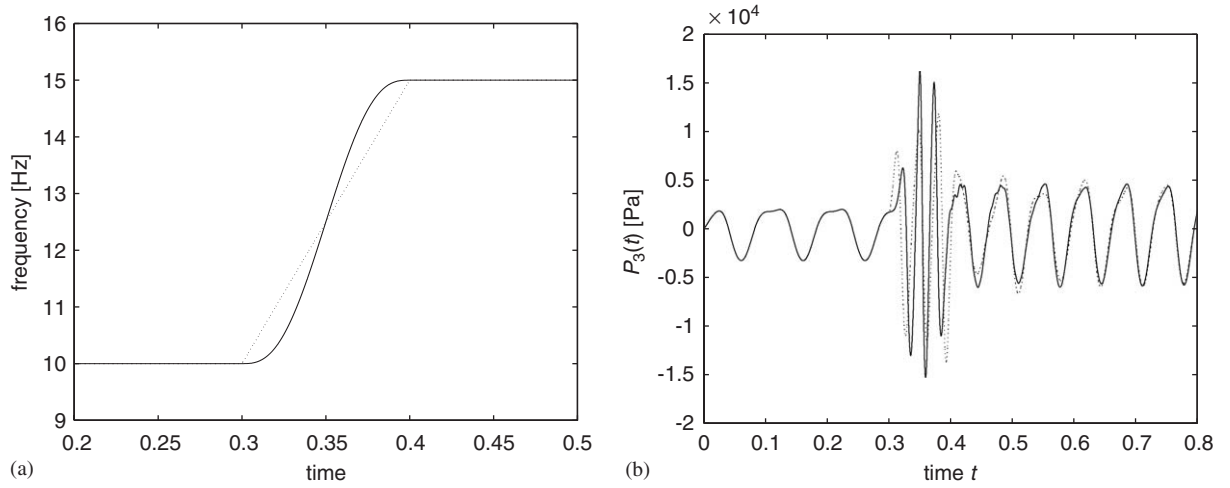

Fig. 21. The sound pressure $p_3(t)$ plotted for different accelerations using the reflection function method. The resonator was a complex muffler. The buffer length was $L_v = 16\,\text{cm}$ and the diameter of the restriction was $d_2 = 3\,\text{cm}$. A continuous, but not continuously differentiable acceleration (dashed) and a five times continuously differentiable, that is smooth, acceleration (solid) are displayed in the same figure. (a) Acceleration of f_0; (b) $p_3(t)$.

solutions are used. To get a better idea of the actual system behaviour, the reflection function method can be used.

Fig. 21 shows the pressure $p_3(t)$ calculated from the reflection function method when a change in fundamental frequency of the piston is applied. The frequency of the piston was held constant at $f_0 = 10\,\text{Hz}$ up to 0.3 s. At $t = 0.3\,\text{s}$ a linear change in frequency was applied until $t = 0.4\,\text{s}$. After that the frequency was again held constant, but now at the new frequency of $f_0 = 15\,\text{Hz}$, see Fig. 21. In the same figure, a smoother acceleration (five timed continuously differentiable) is also plotted. Note that this smooth transition from one constant speed to another gives a smoother change in pressure. In these graphs, the transient behaviour of the system is clear. Each time the fundamental frequency is changed, a new transient solution is created. These

solutions will die out after some system dependent time when the fundamental frequency is held constant once again.

In comparing the two cases in Fig. 21, it is concluded that a smoother acceleration does not necessarily give smaller pressure perturbations, but in general the transient will die out faster.

6. Results and discussion

Among the various methods tested in this paper, only HBM and reflection function method gave stable and convergent results for the model problem. The one-point frequency domain iteration method proposed by Soedel et al. gave divergent solutions in all cases except when an initial value very close to the solutions was chosen. It should however be mentioned that in Refs. [4,6,7] stable solutions were found for a compressor.

The one-point time domain iteration method proposed in Ref. [13] has the same drawbacks as the one-point frequency domain iteration method above. Only divergent solutions were found for this method as well.

For the steady-state periodic regime, the HBM produces faster results than the reflection function method. This allows a more comprehensive parametric study of the system. For transient behaviour, the reflection function method gives a clear advantage compared to the HBM, since all transient behaviour in the system can be found using this method.

In comparing the calculation time, the HBM is generally faster than the reflection function method. For simple systems with low levels, the reflection function requires only a quite large time step. Consequently, in this case the reflection function method is faster, sometimes even faster than the HBM. But for systems with higher levels and larger oscillations, the time step in the reflection function method must be smaller in order to solve the system using some numerical scheme. This is the main reason for the reflection function method being slower compared to the HBM.

A general conclusion can be drawn from the presented graphs in Section 5. The methods seem to give very similar results for simple as well as complex systems with, in some sense, small nonlinearities. As the levels are increased, and the degree of nonlinearity is increased, the solutions slowly diverge. There could be many reasons for this discrepancy. Some of them are summarized below.

Theoretically, the reflection function and the impedance/admittance descriptions of the system are equivalent. For implementation using measured data and discrete time and frequency functions some differences will however occur. For a simple resonator system, the discrepancy is small, for example the infinite cylindrical pipe case used for comparison. When the complexity of the system increases, towards a more realistic case, the discrepancy between the different system descriptions becomes crucial. When taking the inverse Fourier transform of a calculated or measured impedance, a contradiction between the desired features will arise. The reflection function is a fast function by means of a large difference in value over a very short period of time. To model this high frequencies are needed. But when high frequencies are present using an inverse Fourier transform, Gibb's phenomenon will arise. These spurious oscillations do not exist in the physical system, but they arise from the mathematics.

As mentioned above, a more complex system with higher levels and larger oscillations also needs a smaller time step. There will be a compromize between calculation time and accuracy. A small difference between solutions using different time steps could be found. Hence, the size of the time step also influence the comparison between the methods.

A limitation of the presented methods is that there is no direct possibility to take into account nonlinear wave propagation in the models. It would require an approach as for example in Refs. [16–19].

References

[1] H. Bodén, M. Åbom, Modelling of fluid machines as sources of sound in duct and pipe systems, *Acta Acustica* 3 (1995) 549–560.
[2] H. Bodén, F. Albertson, Linearity tests for in-duct acoustic one-port sources, *Journal of Sound and Vibration* 237 (1) (2000) 45–65.
[3] A.D. Jones, Modelling the exhaust noise radiated from reciprocating internal combustion engines—a literature review, *Noise Control Engineering Journal* 23 (1984) 12–31.
[4] W. Soedel, E. Padilla-Navas, B.D. Kotalik, On Helmholtz resonator effects in the discharge system of a two-cylinder compressor, *Journal of Sound and Vibration* 30 (3) (1973) 263–277.

[5] M.L. Munjal, *Acoustics of Ducts and Mufflers*, Wiley Interscience, New York, 1987.
[6] J.P. Elson, W. Soedel, Simulation of the interaction of compressor valves with acoustic back pressures in long discharge lines, *Journal of Sound and Vibration* 34 (2) (1974) 211–220.
[7] R. Singh, W. Soedel, Interpretation of gas oscillations in multicylinder fluid machinery manifolds by using lumped parameter descriptions, *Journal of Sound and Vibration* 64 (3) (1979) 387–402.
[8] H. Bodén, The multiple load method for measuring the source characteristics of time-variant sources, *Journal of Sound and Vibration* 148 (1991) 437–453.
[9] E. Ngoya, J. Rousset, M. Gayral, R. Quere, J. Obregon, Efficient algorithms for spectra calculations in non-linear microwave circuits simulators, *IEEE Transactions on Circuits and Systems* 37 (11) (1990) 1339–1355.
[10] E. Ngoya, A. Suarez, R. Sommet, R. Quere, Probes make simple the steady state analysis of microwave free or forced oscillator and the stability investigation of periodic regimes by harmonic balance, *International Journal of Microwave and Millimeter Wave and Computer-Aided Engineering* 5 (3) (1995) 210–223.
[11] J. Gilbert, J. Kergomard, E. Ngoya, Calculation of the steady state oscillations of a clarinet using the harmonic balance technique, *Journal of the Acoustical Society of America* 86 (1) (1989) 35–41.
[12] F. Albertson, J. Gilbert, Harmonic balance method used for calculating the steady state oscillations of a simple one-cylinder cold engine, *Journal of Sound and Vibration* 241 (4) (2001) 541–565.
[13] V.H. Gupta, On the Flow-Acoustic Modelling of the Exhaust System of a Reciprocating Internal Combustion Engine, Doctoral Thesis, Indian Institute of Science, Bangalore, India, 1991.
[14] K.-Y. Fung, H. Ju, B.P. Tallapragada, Impedance and its time-domain extensions, *AIAA Journal* 38 (1) (2000) 30–38.
[15] B. Gazengel, J. Gilbert, N. Amir, Time domain simulation of single reed wind instrument. From the measured input impedance to the synthesis signal. Where are the traps?, *Acta Acustica* 3 (1995) 445–472.
[16] P.O.A.L. Davies, M.F. Harrison, Hybrid systems for IC engine breathing noise synthesis, *Proceedings of the Institute of Acoustics* 15 (1993) 369–374.
[17] M.F. Harrison, Time and Frequency Domain Modelling of Vehicle Intake and Exhaust Systems, PhD Thesis, I.S.V.R., University of Southampton, 1994.
[18] J.M. Desantes, A.J. Torregrosa, A. Broatch, Hybrid linear/nonlinear method for exhaust noise prediction, SAE Paper-950545, 1995.
[19] F. Payri, J.M. Desantes, A.J. Torregrosa, Acoustic boundary condition for unsteady one-dimensional flow calculations, *Journal of Sound and Vibration* 188 (1) (1995) 85–110.
[20] Y. Özyörük, L.N. Long, A time-domain implementation of surface acoustic impedance condition with and without flow, *Journal of Computational Acoustics* 54 (1997) 277–296.
[21] M.S. Nakhla, J. Vlach, A piecewise harmonic balance technique for determination of periodic response of non-linear systems, *IEEE Transactions on Circuit Theory* 23 (2) (1976) 85–91.
[22] J. Kim, W. Soedel, Convergence of gas pulsation simulations in combined time and frequency domain models, in: *Proceedings of 1990 International Compressor Engineering Conference*, 1990, pp. 641–646.
[23] J.O. Smith, Physical modelling synthesis update, *Computer Music Journal* 20 (2) (1996) 44–56.
[24] D.H. Keefe, Physical modelling of wind instruments, *Computer Music Journal* 16 (4) (1992) 57–73.
[25] J.D. Polack, X. Meynial, J. Kergomard, C. Cosnard, M. Bruneau, Reflection function of a plane sound-wave in a cylindrical tube, *Revue de Physique Appliquee* 22 (5) (1987) 331–337.
[26] S. Nygård, Modelling of low frequency sound in duct networks, Report TRITA-FKT 2000:57, The Marcus Wallenberg Laboratory for Sound and Vibration Research, KTH, Stockholm, Sweden, 2000.
[27] E. Ngoya, R. Larchevèque, Envelop transient analysis: a new method for the transient and steady state analysis of microwave communication circuits and systems, *IEEE MTT-S Digest* (1996) 1365–1368.